Journal of Polymer Research **10:** 7–12, 2003.

Electroluminescence Characteristics of Aromatic Polyimides by Vapor Deposition Polymerization

Shou-Chian Hsu, Wha-Tzong Whang* and Shih-Chia Chen
Institute of Materials Science & Engineering, National Chiao Tung University, 1001 Ta Hsueh Road, Hsin Chu, Taiwan 300, Republic of China
*(*Author for correspondence; Tel.: 886-3-5731873; Fax: 886-3-5724727; E-mail: wtwhang@cc.nctu.edv.tw)*

Received 1 March 2002; accepted in revised form 12 September 2002

Key words: light-emitting diode, polyimide, vapor deposition polymerization (VDP)

Abstract

Light emitting polyimide (PI) thin films are successfully prepared from two kinds of diamines: 2,5-Bis(4-aminophenyl)-l,3,4-oxadiazole (BAO) and 4,4′-(9-Fluorenylidene)dianiline (BAPF) reacting with 4,4′-(Hexafluoroisopropylidene)diphthalic anhydride (6FDA) by vapor deposition polymerization (VDP). We succeed to reduce the thickness of the thin polyimide film to 150 Å, and the threshold voltage of BAO-6FDA and BAPF-6FDA PI light-emitting diodes to 4.5 V and 6.5 V respectively. The root mean square of the surface roughness of the BAO-6FDA and BAPF-6FDA PI films are 8.8 Å and 4.7 Å respectively. But that of the BAO-6FDA film from wet coating process is 37.1 Å. Apparently, VDP process is the better way to produce smooth polyimide film. The BAO-6FDA LED film emits a broader electroluminscence (EL) band, covering the full range of visible light (400 nm to 700 nm), than the BAPF-6FDA LED. However, the electroluminescence efficiency of BAPF-6FDA LED device is better than BAO-6FDA LED device. It is due to the better balance on the hole and electron injection in the former and better intermolecular charge transfer.

Introduction

Polyimides have been applied in a variety of fields, such as the aerospace and automotive industries, alignment layers for liquid crystal displays, interlayer dielectric insulators and the microelectronics industry, because of their excellent mechanical strength, superior thermal and chemical and photic stabilities, good film formability, and planarizability [1–6]. Some research groups have demonstrated significant improvements in photoluminescence (PL) or electoluminescence (EL) by using polyimides as a hole transport material (HTL) [7–12]. Polyimides may also be used as light emitting materials (LED) [13–27]. The published polyimide light emitting materials may contain the moieties of anthracence, or perylene, or metal complex, or tetraphenyl or terabiphenyl-*p*-quinquephenyl, or 2,5-distyrylpyrazine, dibenzofurane, or furyl-substituted biphenylene. Conventionally, a polyimide thin film has been prepared from its soluble precursor polymer solution by spin coating or casting. There are some disadvantages by using these wet processes. It is difficult to remove impurities in monomers and solvents and easily generate microvoids or pinholes in the film [28–33]. These impurities or defects may reduce or destroy the luminescence of the devices. In addition, the film thickness and thickness uniformity are hard to control. The vapor deposition polymerization (VDP) method can overcome the disadvantages of the wet processes. This dry process may generate fewer impurities and the film thickness and surface smoothness can easily be controlled.

There is some research about preparation of polyimide via VDP used in light-emitting diodes. Jou et al. [28] have prepared single-layer molecularly doped electroluminescent polymer by co-evaporating PMDA, ODA, TPD and Alq_3. In this case, polyimide is used as a binder but not an active light emitting material. Kim's group [29] has reported the polyimide as a hole-transporting layer with newly synthesized diamine containing TPD moiety. In this study, we try to study aromatic polyimide as an active light emitting layer in the device. The poly(amic acid)s are prepared from 2,5-Bis(4-aminophenyl)-1,3,4-oxadiazole (BAO) and 4,4′-(9-fluorenyli-dene)dianiline (BAPF) by vapor deposition polymerization with 4,4′-(Hexafluoroisopropylidene)diphthalic anhydride (6FDA). They are then thermally converted into polyimides. Our laboratory has successfully prepared active light emitting polyimides by the wet process. The PIs from 6FDA exhibited lower driving voltage than other common dianhydrides [34]. Oxadiazole-base conjugated polymers are very attractive as active components in light-emitting diodes due to their high electron affinity. Aromatic oxadiazole compound BAO provided the electron-transporting and hole-blocking properties. BAPF is the conjugated materials composed of fluorene and aromatic rings. Fluorene derivatives have shown thermal and chemical stability and high fluoresence quantum yield in the solid state. There-

fore, we expect the PIs from BAPF or BAO with 6FDA to exhibit excellent electroluminescence by vapor deposition polymerization.

Experimental

Materials

The reaction route for the preparation of the polyimides is shown in Scheme 1. 2,5-Bis(4-aminophenyl)-1,3,4-oxadiazole (BAO, 98%) from Lancaster and 4,4′-(9-fluorenylidene)dianiline (BAPF) from Aldrich were dried in a vacuum oven at 120 °C for 3 hours prior to use. 4,4′-(hexafluoro-iso-propylidene)diphthalic anhydride (6FDA) from Aldrich Chemical Co. was purified by recrystallization from acetic anhydride and then dried in a vacuum oven at 125 °C over night.

Vapor Deposition Polymerization and Preparation of Light-Emitting Diodes

Poly(amic acid) films were prepared from two kinds of diamines: 2,5-Bis(4-aminophenyl)-1,3,4-oxadiazole (BAO) and 4,4′-(9-Fluorenylidene)dianiline (BAPF) reacting with 4,4′-(hexafluoro-iso-propylidene) diphthalic anhydride (6FDA) on the precleaned ITO by vapor deposition polymerization. The deposition rate was controlled by the boat temperature. BAO or BAPF and 6FDA were vapor co-deposited on the ITO glass from the Ta boats in a vacuum chamber of 5×10^{-6} torr at the deposition rate of 1 Å/sec. Thermal imidization was then carried out in a furnace at 100 °C for 1 h and 250 °C for 2 h under vacuum. The VDP polyimide thickness are 150 Å, 300 Å, 600 Å and 800 Å. The metal Al was then evaporated onto the surface of the polyimide films to form ITO/PI/Al light-emitting device under 5×10^{-6} torr at the deposition rate of 10 Å/sec.

Characterization

Infrared (IR) spectra were measured with Nicolet Protégé 460. Photoluminescence (PL) spectra of all films were measured using HITACHI F-4500 Spectrofluorophotometer with the excitation source at 355 nm. The UV-Vis spectroscopy was taken with HP8453 UV-Vis spectrometer. The energy level of electronic structure of the polymers was determined from UV-Vis absorption spectra and the data of cyclic voltammetry were measured using CHI600A Electrochemical Analyzer. The cyclic voltammetry was carried out using Pt counter electrode and a Ag/Ag^+ reference at the scan rate of 10 mv/s. The electrolyte was 0.1 M of tert-$BuNClO_4$ in acetonitrile. The results were compared with a ferrocene/ferrocenium (FOC) couple measured in the same solution. The deposition rates and film thickness were monitored by using Maxtek MDC-360 quartz oscillation thickness monitor in deposition. The real thickness was measured by Alpha Step Dektak ST surface profiler. The calibration curve of real thickness vs quartz oscillation thickness was then used in the following deposition to get the correct thickness. The electroluminescence (EL) spectra were measured with a Jasco FR-770 spectrometer. The current-voltage characteristics of the LEDs were measured with a Keithley 237 electrometer. The intensity-voltage characteristics were measured with a Keithley 237 electrometer and a photodiode detector connected with a New Port power meter (Model 1815-C). Atomic force microscopy (AFM) images were obtained using Digital NaroscopeE + AFM at the scan rate of 1 Hz. All measurements were carried out at room temperature.

Results and Discussion

Structure Characterization

Figure 1 shows the FTIR spectra of the polyimide thin films before and after imidization. Both as-deposited films show the absorption peaks at 1850 cm^{-1}, and 1780 cm^{-1} due to the carboxylic anhydride. This indicates the monomers in as-deposited films still remain nonreacted even at the deposition rate ratio of 1 : 1. After imidization, the peaks of the dianhydride at 1850 cm^{-1} and 1780 cm^{-1} disappear, and new absorption peaks at 1780 cm^{-1}, 1720 cm^{-1} and 1380 cm^{-1} appear; these peaks are associated with the characteristic absorption of the imide group. The former two peaks are due to the asymmetric and symmetric C=O stretching and the last peak is associated with the C–N stretching. Judging from the IR spectra, no dianhydride groups are left after imidization.

AFM Images

Figure 2 shows the surface morphology of polyimide films obtained from two different processes, i.e., vapor deposition polymerization and wet coating. For the samples prepared

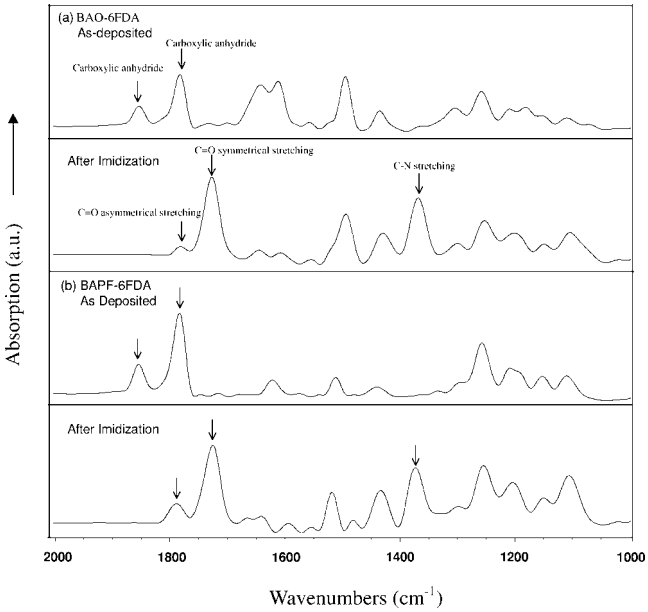

Figure 1. FT-IR spectra of polyimides: (a) BAO-6FDA and (b) BAPF-6FDA before and after imidization.

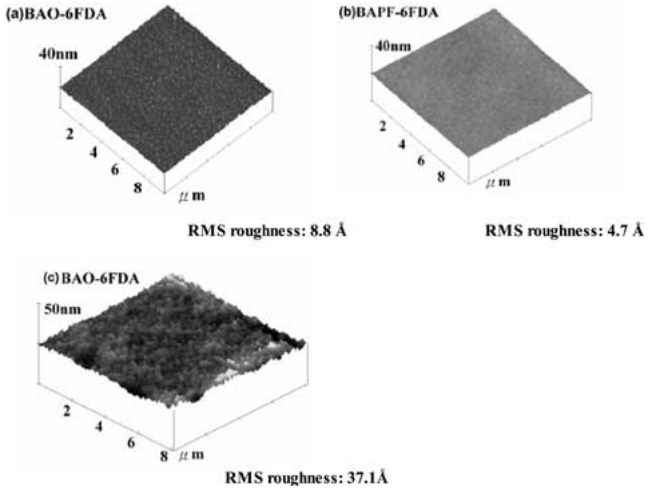

Figure 2. Surface morphology of the polyimides (800 Å): (a) BAO-6FDA and (b) BAPF-6FDA by vapor deposition; (c) BAO-6FDA by wet coating.

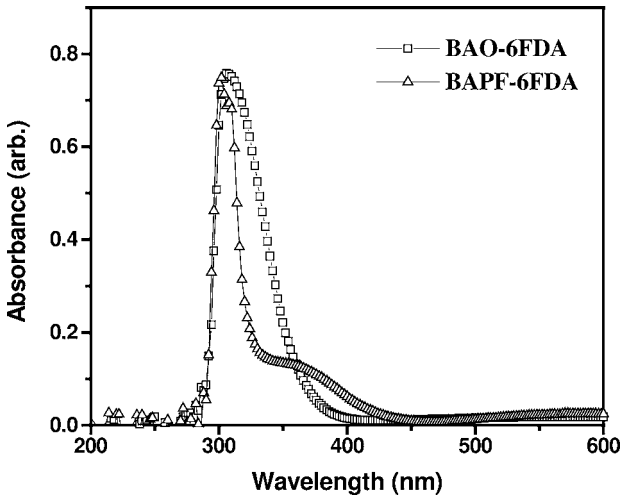

Figure 3. UV-vis absorption spectra of polyimides BAO-6FDA (□) and BAPF-6FDA (△).

by vapor deposition, the root mean-squared (RMS) roughnesses on the BAO-6FDA and BAPF-6FDA PI films (800 Å) are 8.8 Å and 4.7 Å, respectively. For those prepared by wet coating, the RMS roughness on the BAO-6FDA thin film (800 Å) is about 37.1 Å [34]. The VDP PI film has a smaller RMS value of the surface roughness. Apparently VDP process is the better way to produce smooth polyimide thin film than the wet coating process.

UV-Vis Absorption Spectra

Figure 3 shows the UV-Vis absorption spectra of the polyimide films. Absorption of BAO-6FDA ranges from 280 nm to 400 nm with the absorption peak at 306 nm. Absorption of BAPF-6FDA ranges from 280 nm to 450 nm with the absorption peak at 302 nm. The onset of UV-Vis absorption are located at 370 nm and 429 nm for BAO-6FDA and BAPF-6FDA, respectively. The oneset of UV-Vis absorption is used to calculate the energy gap between the highest occupied molecular orbital (HOMO) and the lowest occupied molecular orbital (LUMO). The corresponding energy gaps are 3.35 eV and 2.89 eV, respectively.

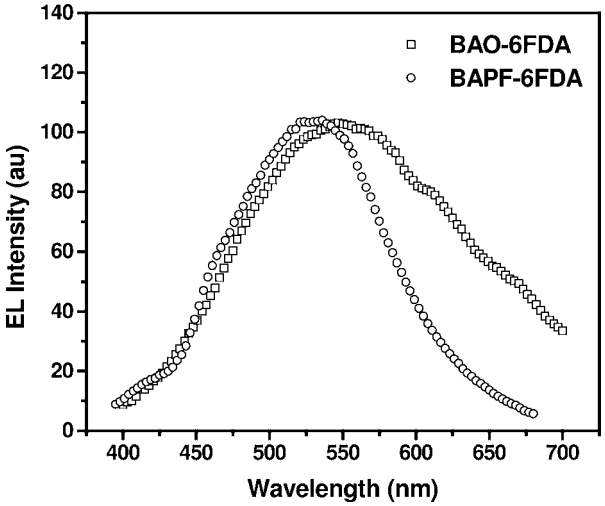

Figure 4. Electroluminescence spectra of polyimide LED devices: ITO/BAO-6FDA(□)/Al, ITO/BAPF-6FDA(○)/Al.

Electroluminescence Spectra

Figure 4 shows the EL spectra of the PI LED ITO/PI/Al for the BAO-6FDA and BAPF-6FDA PI films. Both PI films show broad EL spectra. The emissive peaks are located at 550 nm and 530 nm with the full-width half maximum (FWHM) of 196 nm and 135 nm for BAO-6FDA and BAPF-6FDA PI films, respectively. The emission of BAO-6FDA PI film is broader and shifts towards longer wavelength compared with that of BAPF-6FDA PI film. Both LED devices give uniform light emission when a DC positive voltage is applied to the ITO electrode.

Current Density-Voltage-Brightness (I-V-B) Characteristics

Figures 5 and 6 present the current density-voltage (I-V) and brightness-voltage (B-V) characteristics for single-layer ITO/PI/Al light-emitting diodes with three different PI film thickness. In Figure 5(a), the I-V curves show the characteristics of typical Schottky-type diode. The threshold voltage of ITO/BAO-6FDA/Al single-layer device are about 4.5 V, 6 V and 17 V for thickness of 150 Å, 300 Å, and 600 Å, respectively. ITO/BAPF-6FDA/Al single–layer devices in Figure 6 show the threshold voltage 6.5 V, 8 V and 18 V for thickness of 150 Å, 300 Å and 600 Å respectively. The current density of the second type of the single-layer devices is much lower. The EL efficiency of single-layer devices can be evaluated from the slope of the brightness versus current density in Figure 7. It is found that thicker PI films exhibit higher efficiencies for both types of single-layer devices, and BAPF-6FDA LED has a higher EL efficiency than BAO-6FDA LED although the former has a higher threshold voltage.

Many papers have revealed that wholly aromatic polyimides show a broad fluorescence originating from intermolecular charge transfer (CT) complex [35–39]. The charge at HOMO and LUMO is localized at the electron-donating aminophenyl fragment and the electron-accepting imide fragment. This means charge transfer can occur via the electron HOMO to LUMO transition, and CT can be im-

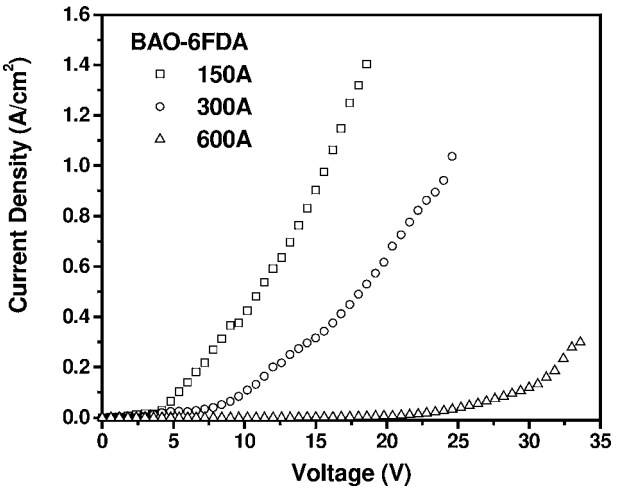

(a)

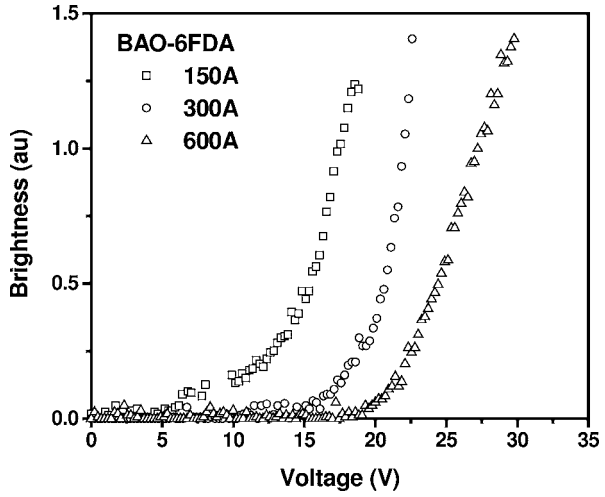

(b)

Figure 5. (a) Current density-voltage and (b) brightness-voltage characteristics of polyimide LED devices ITO/BAO-6FDA/Al with different PI thickness: 150 Å (□), 300 Å (○) and 600 Å (△).

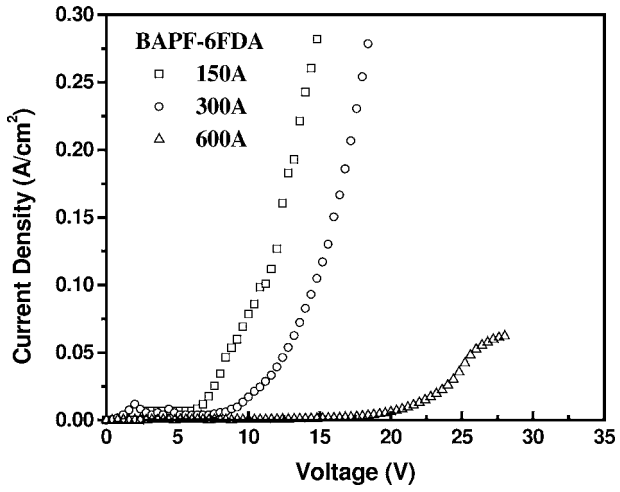

(a)

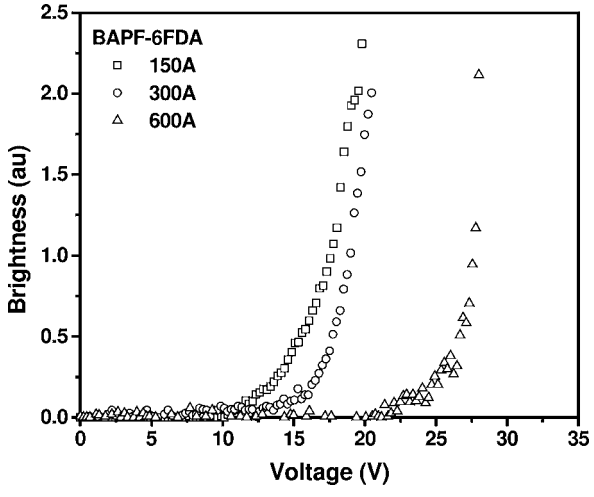

(b)

Figure 6. (a) Current density-voltage and (b) brightness-voltage characteristics of polyimide LED devices ITO/BAPF-6FDA/Al with different PI thickness: 150 Å (□), 300 Å (○) and 600 Å (△).

proved by higher electron-acceptability of dianhydrides and higher electron-donatability of diamines as monomers [38]. The electron-drawing oxadiazole in diamine decreases the electron-donatability of BAO, and also reduces the CT effect. It results in the lower efficiency of BAO-6FDA LED than that of BAPF-6FDA LED. Besides, CT is also affected by the concentration. Increase in concentration leads to increase in the amount of intermolecular CT sites [39]. That could be the reason that thicker PI films show higher EL efficiency. The detailed effects of the CT in PI-LED devices are currently under investigation.

Cyclic Voltammetry Characteristics

Cyclic Voltammetry is a useful tool to study the electrochemical properties and energy level of charge transport materials. Figure 8 shows the cyclic voltammograms of polyimide thin films. For BAPF-6FDA and BAO-6FDA PI, the onset of oxidation (E_{ox}) occurred at 1.04 V and 1.71 V respectively, and the onset of reduction (E_{re}) occurred at −1.64 V and −1.48 V respectively. The energy levels of the

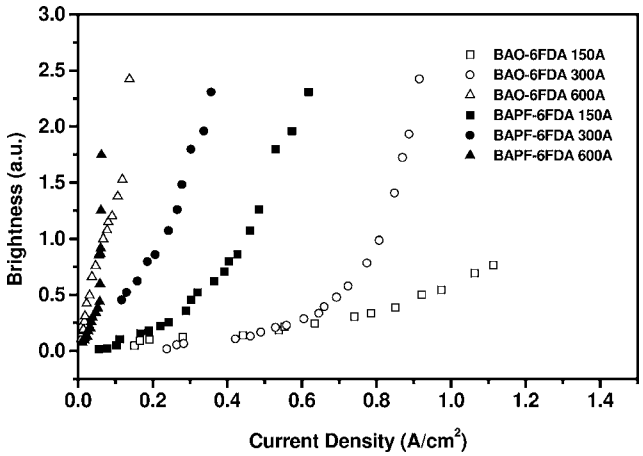

Figure 7. Brightness-current density characteristics of polyimides LED devices with different PI thickness: ITO/BAO-6FDA/Al, 150 Å (□), 300 Å (○) and 600 Å (△); ITO/BAPF-6FDA/Al, 50 Å (■), 300 Å(●) and 600 Å (▲).

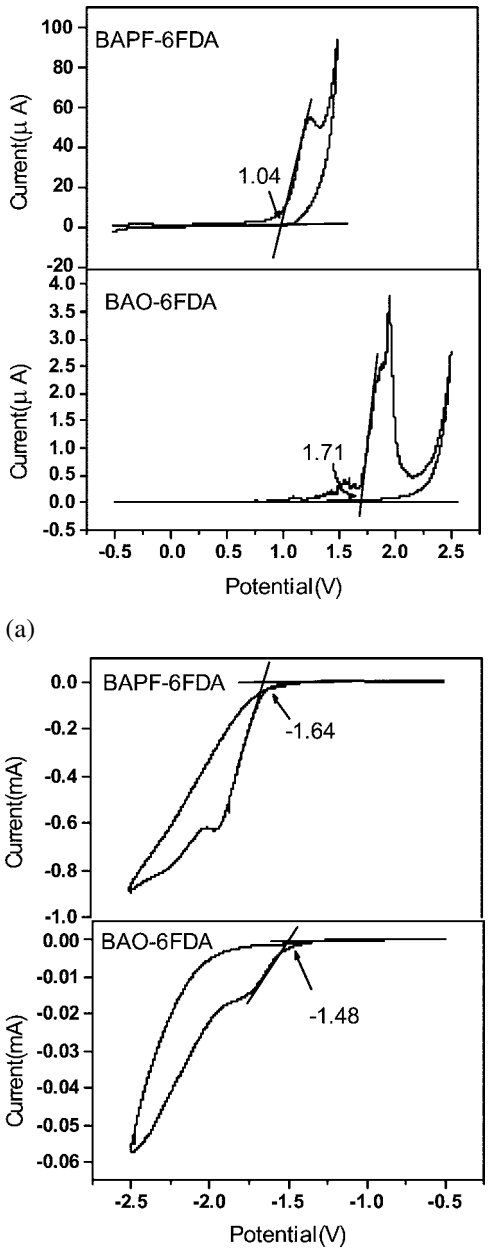

Figure 8. Cyclic voltammograms of polyimides: (a) oxidation curves; (b) reduction curves.

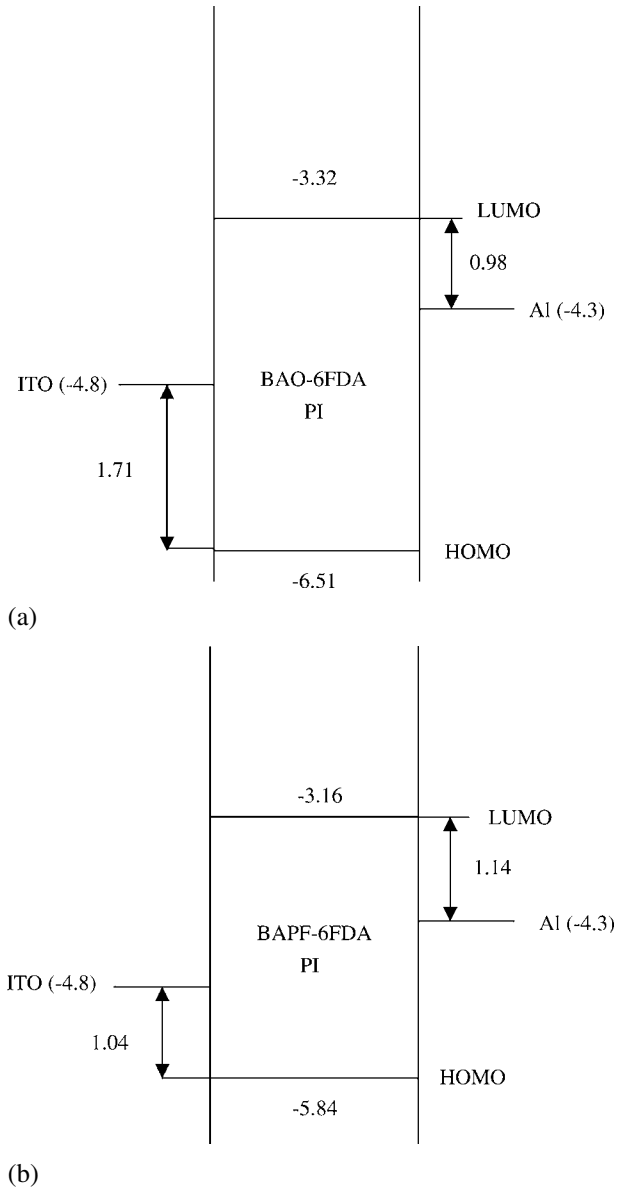

Figure 9. Band diagrams of: (a) ITO/BAO-6FDA/Al and (b) ITO/BAPF-6FDA/Al.

polyimides can be estimated from the following equation:

$$\text{HOMO} = (-4.8 - E_{\text{ox}})\,\text{eV},$$

$$\text{LUMO} = (-4.8 - E_{\text{re}})\,\text{eV},$$

where the constant -4.8 is the energy level of ferrocence related to the vacuum level [40]. The energy levels of two PI LED are displayed in Figure 9 and summarized in Table 1. The energy levels of the highest occupied molecular orbital (HOMO) and the lowest unoccupied molecular orbital (LUMO) are -6.51 eV and -3.32 eV referred to the vacuum level for BAO-6FDA PI; -5.84 eV and -3.16 eV for BAPF-6FDA PI. It indicates that BAO-6FDA PI has a lower electron injection barrier than BAPF-6FDA PI due to the electron transporting oxadiazole unit. On contrast, BAPF-6FDA PI has a lower hole injection barrier than BAO-6FDA PI. It is due to more hole transporting arylene structure in BAPF-6FDA polyimide. Compared the energy barrier to each electrode for both LED devices, ITO/BAPF-6FDA/Al LED exhibits the more balanced charge injection from the two electrodes (1.14 eV and 1.04 eV) than ITO/BAO-6FDA/Al LED. The energy barriers of the ITO/BAO-6FDA interface and the BAO-6FDA/Al interface are 1.71 eV and 0.98 eV respectively. Hole injection is more difficult than electron injection in this device. The electron injection and the hole injection become imbalanced. Thus, the EL efficiency of BAO-6FDA is lower than that of BAPF-6FDA LED.

Conclusions

Light emitting thin aromatic polyimide films have been successfully prepared by vapor deposition polymerization

Table 1. Electrochemical potentials and energy levels of the polyimides.

Polymer	E^{ox}_{onset} vs E_{FOC} (eV)	E^{red}_{onset} vs E_{FOC} (eV)	HOMO (eV)	LUMO (eV)	E_{gap} (eV)
BAO-6FDA	1.71	−1.48	−6.51	−3.32	−3.19 (−3.35[a])
BAPF-6FDA	1.04	−1.64	−5.84	−3.16	−2.68 (−2.89[a])

[a] E_{gap} stand for the band gap energy estimated from the onset wavelength of the optical absorption.

(VDP) from diamine BAO and BAPF with dianhydride 6FDA. Using VDP process, more smooth surface morphology of the LED devices can be obtained than using wet coating process. Effective active PI LED can be performed as low as 150 Å of PI thickness. The threshold voltage of the LED decreases with decreasing thickness, which can be as low as 4.5 V. Both BAO-6FDA and BAPF-6FDA single-layer LED devices show broad EL spectra. Thicker PI film exhibit higher efficiencies in both types of LEDs. It could be resulted from the more CT sites in the thicker PI film then increasing the intermolecular CT. BAPF-6FDA LED has a higher EL efficiency than BAO-6FDA LED because of the more balanced charge injection from both electrodes of the former device and the stronger intermolecular CT.

Acknowledgement

The authors gratefully acknowledge the National Science Council of the Republic of China and the Lee and MTI center in NCTU for the financial support of this work under Grant NSC 90-2216-E-009-015 and the research on photonic devices and modules project respectively.

References

1. M. K. Ghosh and K. L. Mittal, *Polyimides: Fundamentals and Applications*, Marcel Dekker, New York, 1996.
2. H. Icil and S. Icil, *J. Polym. Sci. A: Polym. Chem.*, **35**, L2137 (1997).
3. D. Wilson and P. Hergenrothe (Ed. H. D. Stenzenberger), *Polyimides*, Chapmam & Hall, London, 1990.
4. S. L. Jwo, W. T. Whang and W. C. Liaw, *J. Appl. Polym. Sci.*, **74**, 2832 (1999).
5. S. L. Jwo, W. T. Whang, T. E. Hsich, F. M. Pan and W. C. Liaw, *J. Polym. Res.*, **6**, 175 (1999).
6. M. H. Tsai and W. T. Whang, *Polymer*, **42**, 4197 (2001).
7. Y. F. Wang, T. M. Chen, K. Okada, M. Uekawa, T. Nakaya, M. Kitamura and H. Inoue, *J. Polym. Sci.: Polym. Chem.*, **38**, 2032 (2000).
8. Y. Kim, J. G. Lee, K. J. Han, H. K. Hwang, D. K. Choi, Y. Y. Jung, J. H. Keum, S. Kim, S. S. Park and W. B. Im, *Thin Solid Films*, **363**, 263 (2000).
9. J. G. Lee, S. Kim, D. K. Choi, Y. Kim, S. C. Kim, M. I. Lee and K. Jeong, *Kor. Phy. Soc.*, **35**, S604 (1999).
10. H. O. Ha, W. J. Cho and C. S. Ha, *Mol. Cryst. Liq. Cryst.*, **349**, 443 (2000).
11. J. G. Lee, Y. Kim, S. H. Jang, S. N. Kwon and K. Jeong, *Appl. Phys. Lett.*, **72**, 1757 (1998).
12. E. I. Maltsev, M. A. Brusentseva, V. A. Kolesnikov, V. I. Berendyaev, B. V. Kotov and A. V. Vannikov, *Appl. Phys. Lett.*, **71**, 3480 (1997).
13. W. Y. Ng, X. Gong and W. K. Chan, *Chem. Mater.*, **11**, 1165 (1999).
14. Y. F. Wang, T. M. Chen, K. Okada, M. Uekawa, T. Nakaya, M. Kitamura and H. Inoue, *J. Poly. Sci. A: Polym. Chem.*, **38**, 2032 (2000).
15. Y. Kim, J. G. Lee, D. K. Choi, Y. Y. Jung, B. Park, J. H. Keum and C. S. Ha, *Synth. Met.*, **91**, 329 (1997).
16. E. I. Mal'tsev, M. A. Brusentseva, V. A. Kolesnikov, V. I. Berendyaev, B. V. Kotov and A. V. Vannikov, *Appl. Phys. Lett.*, **71**, 3480 (1997).
17. E. I. Mal'tsev, M. A. Brusentseva, V. A. Kolesnikov, V. I. Berendyaev, B. V. Kotov, A. V. Vannikov, A. R. Tameev and A. A. Kozlov, *Polym. Int.*, **42**, 404 (1997).
18. P. Posch, M. Thelakkat and H. W. Schmidt, *Synth. Met.*, **102,** 1110 (1999).
19. S. M. Pyo, S. I. Kim, T. J. Shin, M. Ree, K. H. Park and J. S. Kang, *Polym.*, **40**, 125 (1998).
20. E. I. Mal'tsev, M. A. Brusentseva, V. A. Kolesnikov, V. I. Berendyaev, B. V. Kotov, A. V. Vannikov and A. A. Kozlov, *Mendeleev. Commun.*, 31 (1998).
21. H. Icil and H. Icil, *J. Polym. Sci. A: Polym. Chem.*, **35**, 2137 (1997).
22. W. Lu, J. P. Gao, Z. Y. Wang, Y. Qi, G. G. Sacripante, J. D. Duff and P. R. Sundararajan, *Macromolecules*, **32**, 8880 (1999).
23. H. O. Ha, W. J. Cho and C. S. Ha, *Mol. Cryst. and Liq. Cryst.*, **349**, 443 (2000).
24. S. M. Pyo, S. I. Kim, T. J. Shin, M. Ree, K. H. Park and J. S. Kang, *Macromolecules*, **31**, 4777 (1998).
25. I. K. Spiliopoulos and J. A. Mikroyannidis, *Macromolecules*, **31**, 515 (1998).
26. Y. Kim, J. G. Lee and S. Kim, *J. Korean Phys. Soc.*, **35**, S267 (1999).
27. A. Kukhta, E. Kolesnik, M. Taoubi, D. Drozdova and N. Prokopchuk, *Synthetic. Met.*, **119**, 129 (2001).
28. W. K. Wen, J. H. Jou, H. S. Wu and C. L. Chen, *Macromolecules*, **31**, 6515 (1998).
29. J. G. Lee and S. Kim, *J. Korean Phys. Soc.*, **35**, S604 (1999).
30. W. K. Wen, J. H. Joe and J. F. Chiou, *Appl. Phys. Lett.*, **71**, 1302 (1997).
31. H. Yanagisita, D. Kitamoto, K. Haraya, T. Nakane, T. Tsuchiya and N. Koura, *J. Membrane Sci.*, **136**, 121 (1997).
32. S. Ukishima, M. Iijima, M. Sato, Y. Takahashi and E. Fukada, *Thin Solid Film*, **308**, 475 (1997).
33. G. Maggioni, S. Carturan, D. Boscarino, G. Dellamea and U. Pieri, *Mater. Lett.*, **32**, 147 (1997).
34. C. S. Chao, W. T. Whang and S. C. Hsu (in preparation).
35. M. Hasegawa, I. Mita, M. Kochi and R. Yokota, *Polymer*, **32**, 3225 (1991).
36. E. D. Wachsman and C. W. Frank, *Polymer*, **29**, 1191 (1988).
37. J. P. Lafamina and S. A. Kafafi, *J. Phys. Chem.*, **97**, 1455 (1993).
38. M. Hasegawa and K. Horie, *Prog. Polym. Sci.*, **26**, 259 (2001).
39. H. Luo, L. Dong, H. Tang, F. Teng and Z. Feng, *Macromol. Chem. Phys.*, **200**, 629 (1999).
40. Z. Peng, Z. Bao and M. E. Galvin, *Chem. Mater.*, **10**, 2086 (1998).